Available online at www.sciencedirect.com
ScienceDirect
Journal of Magnetic Resonance 187 (2007) 199–204
JMR Journal of Magnetic Resonance
www.elsevier.com/locate/jmr

Time-of-flight variant to image mixing of granular media in a 3D fluidized bed

D.J. Holland *, C.R. Müller, J.F. Davidson, J.S. Dennis, L.F. Gladden, A.N. Hayhurst, M.D. Mantle, A.J. Sederman

Department of Chemical Engineering, University of Cambridge, Pembroke Street, Cambridge CB2 3RA, UK

Received 19 December 2006; revised 5 April 2007
Available online 30 April 2007

Abstract

This paper describes a variant of time-of-flight magnetic resonance (MR) imaging that provides a method of measuring the inherent mixing in a fluidized bed without the introduction of tracer particles. The modifications to conventional time-of-flight imaging enable the measurement of the axial mixing of a precisely controlled initial particle distribution, thereby providing measurements suitable for a direct comparison with models of solids mixing in granular systems. The imaging sequence is applied to characterize mixing, over time scales of 25–1000 ms, in a gas-fluidized bed of Myosotis seed particles; mixing over short timescales, inaccessible using conventional tracer techniques, is studied using this technique. The mixing pattern determined by this pulse sequence is used in conjunction with MR velocity images of the motion of the particles to provide new insight into the mechanism of solids mixing in granular systems.

PACS: 45.70.-n; 47.55.Lm; 83.85.Fg

Keywords: Granular flow; MRI; Solids mixing; PFG; Velocity imaging

1. Introduction

Analysis of conventional studies of the mixing of tracer particles in a gas-fluidized bed is complicated by the influence of the method of introduction of the tracer, and the reproducibility of this procedure, and segregation effects arising from differences in size and density of the tracer compared to the particles comprising the bed. Furthermore, granular systems are opaque and thus not well suited to study using optical techniques, where observations are confined to the region of the wall [1]. The opacity of granular systems also makes direct observations of short time scale mixing processes, such as the drift and wake effects induced by bubble motion in gas-fluidized beds, nearly impossible in three-dimensional systems using conventional tracer studies. Such measurements are essential for the elucidation of the mechanisms of particle mixing in gas–solid fluidized beds [2,3]. This paper presents a novel variant of a time-of-flight magnetic resonance (MR) technique that can be used to overcome these problems, and therefore provide unique insights into granular dynamics within fluidized beds.

Techniques previously employed to make measurements in the core of a fluidized bed include electrical resistance measurements [4], positron emission particle tracking (PEPT) [5], electrical capacitance tomography (ECT) [6], and X-ray photography [7]. In contrast to these techniques, the MR signal can be encoded for displacement, as well as position, and can therefore yield complementary information on the motion and position of granular materials in the same sample environment. This versatility makes MR unique among the three-dimensional tomographic techniques that have been applied to the study of granular systems.

* Corresponding author.
E-mail address: djh79@cam.ac.uk (D.J. Holland).

1090-7807/$ - see front matter © 2007 Elsevier Inc. All rights reserved.
doi:10.1016/j.jmr.2007.04.013

MR has previously been applied to study the motion and mixing of solids in a variety of granular systems. In particular, time-of-flight imaging has been employed to study mixing in rotating cylinders [8] and the dynamics of vibro-fluidized beds [9,10]. However, these approaches have not been successfully employed to study motion in gas-fluidized beds. A major reason for this is that in the case of a gas-fluidized bed the particle number density distribution (i.e., voidage) and particle velocity change significantly during the passing of each bubble (~100 ms), making the application of MR to study motion in these systems particularly challenging. The MR signal of solid particles is also typically characterized by short T_1 and T_2, and very short (<1 ms) T_2^* relaxation times. MR has been successfully implemented in a gas-fluidized bed to image the stable jet structures near the distributor [11] and the gas dynamics in both one- [12] and two-dimensions [13]. Two MR approaches have also been demonstrated for measuring mixing and dispersion in gas-fluidized beds. First, pulsed field gradient (PFG) MR measurements of the displacement probability distribution, or propagator, have been reported [14,15]. However, in a fluidized bed particles move both up and down the bed with speeds ranging over an order of magnitude. Thus, it is difficult to fully characterize the entire velocity distribution with this technique. Furthermore, conventional PFG MR measurements of gas-solid fluidized beds require large magnetic field gradients (>0.1 T m^{-1}) applied in a wide bore (diameter ~10 cm) magnet environment, as well as long acquisition times (~hours). The second approach has utilized ultra-fast FLASH profiles of the axial distribution of a small quantity of poppy seed tracer particles introduced to the top surface of a bed of MR-inert particles [16]. However, as with all tracer studies, these ultra-fast measurements are not well suited to studying the intrinsic mixing of a fluidized bed because it is difficult to insert a well-defined pulse of tracer particles into a fluidized bed instantaneously. The measurements also suffer from a low signal-to-noise ratio, since only a relatively small number of particles are MR-active. In this paper, a novel MR technique is described that utilizes the ability of MR to label particles *in situ* and therefore provides an unambiguous characterization of the intrinsic mixing in a fluidized bed. The technique incorporates modifications to conventional time-of-flight imaging that enable the measurement of particle displacement over observation times between 25 and 1000 ms in a gas-fluidized bed. Thus, the technique can be used to examine short time-scales (~ms) that would be inaccessible to conventional tracer mixing studies. The technique may be compared with other time-of-flight imaging techniques (e.g., [17,18]). However, these techniques are unsuited to the study of motion in a continuously bubbling gas-fluidized bed, due to the dominance of image artefacts or to their inability to access short time-scale mixing. A particular challenge is to quantitatively measure particle displacements in the environment of a changing spin-density distribution that arises from the passage of bubbles. The modifications to conventional time-of-flight imaging developed in this work overcome this problem to enable the measurement of particle displacements in a freely bubbling gas-fluidized bed. These measurements are the first quantitative measurements of this locally induced particle motion in a gas-fluidized system without the use of tracer particles.

2. Experimental

The experimental setup is detailed in Fig. 1. The fluidized bed (40×10^{-6} m^3 slumped volume) was contained within an acrylic tube (i.d. 44 mm, o.d. 60 mm) placed vertically within the MR equipment. Dried air was supplied by a compressor and regulated to 100 kPa before passing to a rotameter, which was used to control the flow rate. The distributor was a porous glass frit; the pressure drop across the distributor was at least equal to that across the bed for typical fluidization velocities, thereby ensuring even fluidization [19]. The particles used in this work were Myosotis seeds (Sutton Seeds Ltd., UK). These particles contain oil, which has relatively long T_1 and T_2 relaxation times (~430 and ~100 ms, respectively), thereby making them easily detected by MR. The seeds were characterized by a diameter and bulk density of ~0.9 mm and ~900 kg m^{-3}, respectively. The minimum fluidization velocity of the particles (U_{mf}) was 0.19 m s^{-1} at ambient conditions.

MR experiments were performed using a Bruker DMX 200 spectrometer operating at a proton (^{1}H) frequency of 199.7 MHz. A birdcage radio frequency (r.f.) coil (i.d. 64 mm) was situated around the outside of the fluidized bed and was used to excite and detect the seeds. Spatial resolution was achieved using a 3-axis shielded gradient system capable of producing a maximum magnetic field

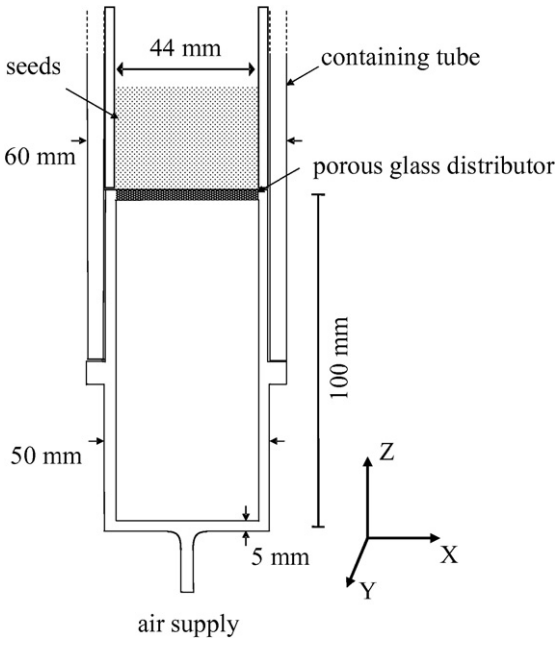

Fig. 1. Sketch of the distributor and bed of seeds within the outer containing tube.

gradient of 0.139 T m^{-1}. The axial spatial resolution of the selective MR imaging sequence was set at 0.625 mm. The mixing times used were between 25 and 1000 ms. The number of averages required to obtain quantitative measurements of the mixing varied depending on the time over which the mixing was observed, as discussed in the following paragraphs. Thus, the total acquisition time for a single observation was between 25 and 110 min, depending on the mixing time of interest.

The novel variant on a time-of-flight MR imaging sequence developed in this work to characterize mixing is shown in Fig. 2. The technique is a selectively refocused one-dimensional imaging sequence, which is related to the 13-interval alternating pulsed gradient stimulated echo (APGSTE) sequence [20], but with important differences. In an APGSTE sequence, the displacement of the particles is encoded in the phase of the magnetization. By contrast, in the sequence presented in Fig. 2, the magnetization associated with particles within a transverse slice of the bed is selectively refocused using a shaped r.f. pulse to provide the population of particles to be observed in the experiment. However, the MR signal associated with the particles is not phase encoded. MR signal from particles that were not in the refocussed slice will be dephased by the slice gradient (G_z), and are therefore invisible in the experiment. Following excitation of the initial tracer distribution, these particles are then allowed to mix for a time period Δ. A read gradient is then applied to recover the position of the particles that comprised the initially excited population. Thus, unlike a PFG experiment, the new technique can be used in direct analogy to conventional tracer mixing studies, but with the advantage that no tracer material is required. A slice selective refocusing r.f. pulse was used in preference to slice selective excitation, as this was found to produce a more uniform initial distribution of particles whose displacement is to be followed. The position, shape and width of the initial distribution of particles can be precisely controlled by adjusting the slice gradient strength and r.f. excitation frequency and shape. The APGSTE-type protocol was used because of the well documented advantages of this approach. First, it allows longer mixing times than a conventional spin–echo sequence, since during the time period Δ the particles will undergo T_1, as opposed to T_2, relaxation. The T_1 relaxation time of the Myosotis seed particles used in this work was 430 ms, which is approximately $4T_2$. Second, the use of the 13-interval sequence refocuses the effects of signal attenuation due to motion in heterogeneous B_0 fields.

A single acquisition using this sequence will measure all magnetization along z at the end of the mixing time Δ. This magnetization will comprise of both the magnetization labelled by the soft refocussing pulse, and unwanted magnetization that has recovered along z during the period Δ. Conventionally, MR is applied to relatively stable systems, such as flow through a packed bed of particles. Unwanted magnetization arising from T_1 relaxation during the mixing time is then overcome by phase cycling the r.f. pulses. However, fluidized beds are inherently dynamic systems (in this system gas bubbles pass every ~100 ms), so it is unlikely that the axial spin distribution arising from two sequential averages will be identical. Therefore the phase cycle used should be as simple as possible, such that, with sufficient repetitions of the sequence, a limiting, time-averaged behaviour will eventually be reached. The number of steps in the phase cycle can be reduced by noting that the major source of unwanted magnetization arises from magnetization excited and refocused by the combination of the final π/2–π r.f. pair. The magnitude of the signal arising from this pair of r.f. pulses will increase as the mixing time Δ increases. To eliminate this signal a two-step phase cycle is required. A measure of the unwanted signal is provided by the deviation from a T_1 decay in a plot of the total signal intensity as a function of mixing time. Fig. 3 shows how the total signal intensity varies with increasing number of averages. It can be clearly seen that for fewer than 1000 averages the signal intensity does not decay exponentially with T_1. As the number of averages increases the decay approaches the expected exponential decay. For more than 1000 averages, the signal intensity follows a T_1 decay for mixing times $\leqslant$400 ms, as shown by the solid line in Fig. 3. For longer mixing times, more averages are required. For example, for 2600 averages the signal decays with the T_1 relaxation to within ±5% for mixing times up to ~800 ms.

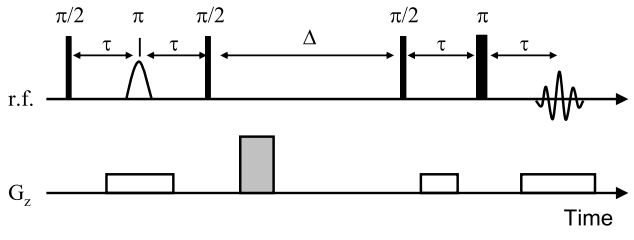

Fig. 2. Pulse sequence for imaging intrinsic mixing. The first π pulse is a shaped excitation pulse which selectively refocuses spins in a horizontal slice at an axial position determined by the frequency of that pulse; a Gaussian π pulse is used. The shaded gradient is a homospoil pulse. The z-direction is vertical and aligned with the magnetic field, B_0.

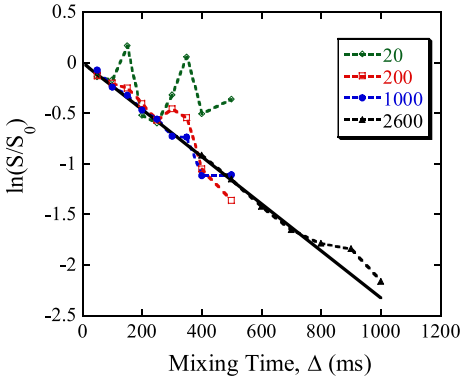

Fig. 3. The effect of increasing the number of averages on the total normalised signal intensity. The solid line represents an exponential T_1 decay with a time constant of 430 ms.

To compare with the data obtained from this new imaging sequence, images of the bulk motion of the solid particles were obtained using a slice-selective, spin–echo pulse sequence with phase-difference velocity encoding [21]. Two increments of the velocity gradient were used. The images were acquired in the axial plane (x–z) with 128×128 voxels and a field of view of 55 mm × 70 mm; this resulted in an in-plane resolution of 0.43 mm × 0.55 mm. A slice thickness of 5.0 mm was used. Forty averages were acquired resulting in a total acquisition time of ~30 min. The raw data were first Fourier-transformed and then processed using in-house software to give a quantitative map of the velocity of the particles.

3. Results

An example of the displacement distribution resulting from an initial excitation applied to a transverse slice section 20 mm above the distributor is shown in Fig. 4; data are shown for a superficial gas flow rate of $U/U_{mf} = 2.0$. These experiments were each acquired with 1000 averages in a time of 25–35 min, depending on the mixing time, Δ, used. It is seen that for a mixing time of 25 ms the distribution is narrow and approximately symmetrical. In this case, the shape of the initial distribution is Gaussian reflecting the choice of the shape of the r.f. refocusing pulse. At longer mixing times, the main peak is seen to distort and travel down the bed towards the gas distributor, while a second peak is seen to appear at a height of 27 mm. A conventional spin–echo axial profile of the signal intensity, and hence particle distribution, revealed that when fluidized the time-averaged position of the top of the bed was 27 mm above the distributor. Thus, the second peak is attributed to particles that have reached the top of the bed during the mixing time.

The reproducibility of the experiments is confirmed in Fig. 5, where three different experiments, each of 1000 averages, are shown for mixing times of 25, 150 and 300 ms. It is interesting to note that changing the location of the selective excitation from 20 mm above the distributor (Fig. 4) to 16 mm (Fig. 5) alters the shape of the resulting 'tracer' distribution. In Fig. 5 a second peak is apparent at a mixing time of 150 ms and persists up to 300 ms, the longest time shown. By contrast, in Fig. 4, while a second peak is seen at 150 ms, the profiles at 300 and 500 ms no longer show a distinct second peak. Instead, the signal is nearly constant, and non-zero, in the region from the top of the bed down to the main peak in the distribution. Preliminary results indicate that this is consistent with the predictions of a counter-current back-mixing model [22], confirmation of this is the subject of ongoing work.

Fig. 6 shows an image of the time-averaged velocity of the solids in the fluidized bed at $U/U_{mf} = 2.0$ and acquired over a period of ~30 min. In Fig. 6 the particles in the center of the bed tend to flow upwards and particles at the

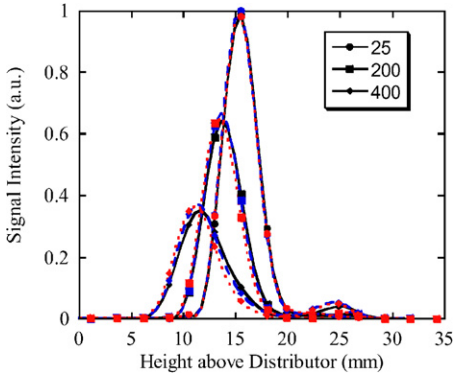

Fig. 5. A plot of three repetitions each at mixing times of 25, 150 and 300 ms for Myosotis seeds at $U/U_{mf} = 2.0$. Each experiment was averaged over 1000 acquisitions. The excitation position was 16 mm above the distributor. The intensity has been adjusted according to the T_1 weighting. The three different colours refer to the three separate experiments performed for each mixing time.

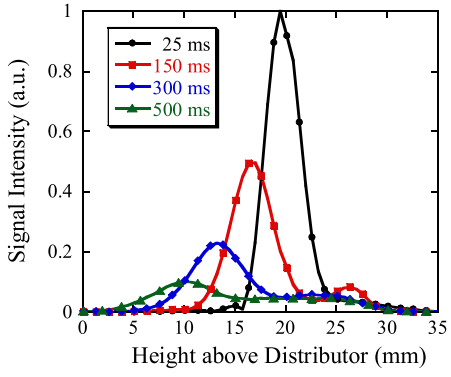

Fig. 4. Plots of signal intensity in arbitrary units showing the relative number of tracer particles at different heights above the distributor, as measured by the MR sequence shown in Fig. 2 for mixing times of 25, 150, 300 and 500 ms and $U/U_{mf} = 2.0$. The signal intensity is the raw signal intensity and has not been adjusted for T_1 weighting. The excitation position was 20 mm above the distributor.

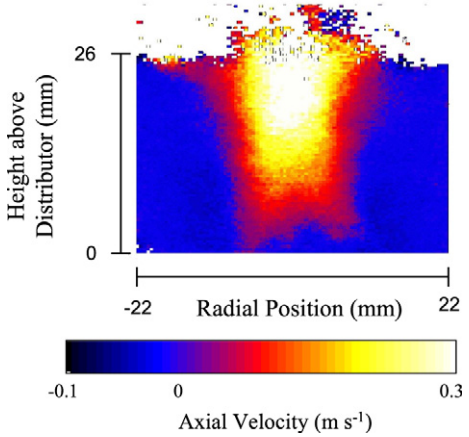

Fig. 6. Image showing the velocity of the solids in a bed of pure Myosotis seeds at $U/U_{mf} = 2.0$. The image was time-averaged over a period of 30 min. The in-plane resolution was 0.43 mm (x) × 0.55 mm (z), with a slice thickness of 5 mm.

walls tend to flow downwards. The region near the distributor shows minimal net upwards movement. The time-averaged upwards velocity tends to increase with height and has an approximately parabolic radial profile. By contrast, the velocity in the downwards flowing regions showed only minor variations with axial and radial position. These spatial variations in the time-averaged velocity are most likely related to both the size and frequency of the bubbles at different locations in the bed, and are a feature of further study.

Comparison of a velocity image, such as that shown in Fig. 6, with the data provided by the new pulse sequence demonstrates that the data are consistent, and that the combination of the two techniques provides greater insight into the dynamics of granular systems. In analyzing these images it should be noted that the velocity images and the displacement distribution of the mixing process are measurements of the short time scale particle motion that is time-averaged over a period of 25–35 min. Looking first at the data in Fig. 6, the mean velocity of the solids with negative (i.e., downwards) velocity was $-0.019\ \mathrm{m\ s^{-1}}$. By comparison, the downwards velocity of the particles associated with the main peak in Fig. 4 can be extracted from the change in the mean position of the peak as a function of time. This yields a value of $-0.020 \pm 0.001\ \mathrm{m\ s^{-1}}$, in excellent agreement with the data in Fig. 6.

There are two possible explanations for the appearance of a second peak in the distribution of particles shown at longer mixing times. First, some material in the initial distribution of particles will be in the central, upward moving region shown in Fig. 6 and, therefore, its motion determined by the macroscopic flow pattern characterizing the bed. Second, material initially moving down the bed may be caused to move up the bed by the passing gas bubbles. By comparing the data obtained from the MR velocity imaging and the 'mixing' pulse sequence, we can elucidate the relative importance of these two phenomena. The fraction of material that was moving up the bed in the initial excitation is estimated from a mass balance on the velocity image shown in Fig. 6. This indicates that the fraction of material in the initial excitation that is moving up the fluidized bed is ~16%. From the results shown in Fig. 5, the fraction of the total signal associated with the population of particles towards the top of the bed at a mixing time of 150 ms is 4%, and by 300 ms it represents 13%. This suggests that over these time scales this sub-population of particles is associated with the macroscopic flow pattern shown in Fig. 6. However, for the data shown in Fig. 4, the fraction of signal associated with heights above the distributor greater than that at which the main peak in the signal intensity distribution occurs is seen to increase to ~40% by 500 ms. This value far exceeds that associated with the particles transported within the central, upward moving section of the bed. We suggest that the additional particles are associated with material initially traveling down the bed which is then caused to travel up the bed before reaching the distributor. The rate of change of velocity of this material will depend on the bubble dynamics in the fluidized bed and the particle motion induced by each bubble.

It is widely accepted that the particle velocity pattern and mixing characteristics in a gas-solid fluidized bed will be determined by the short-time solids mixing processes induced by bubble motion. Three processes, drift, wake and return flow, have been identified that contribute to particle motion following the passage of a bubble [2]. Of these the drift and wake flows are associated with upwards particle motion and the return flow with downwards motion. In order to determine the effect of these processes on mixing in a fluidized bed, direct measurements of the short time scale mixing are required; these cannot be obtained in a three-dimensional bed using conventional tracer techniques. The pulse sequence reported here provides the first direct measure of the return flow of particles in a bubbling fluidized bed, as can be seen from the downward motion of the peak in the signal intensity seen in Figs. 4 and 5. The skew observed in these distributions is also consistent with a population of the particles demonstrating return flow [3]. The signal appearing near the top surface of the bed has its origin in the drift and wake processes. A complete analysis of these processes requires knowledge of the size, frequency and velocity of the gas bubbles. Further research combining this new mixing sequence with studies of the rise and coalescence of gas bubbles [12] will provide a quantitative measure of the contribution of each of these processes to the mixing of particles in continuously operated three-dimensional fluidized beds.

4. Conclusions

In this paper, a modification of time-of-flight imaging has been presented that overcomes artefacts associated with conventional imaging in gas-fluidized beds to yield quantitative information on the particle mixing. The imaging technique described does not require any tracer particles, eliminating the problems associated with tracer injection and segregation. The technique measures the displacement from a precisely controlled initial distribution, and thus is directly comparable with modeling and simulation results. Because the technique does not require a tracer, it is relatively simple to acquire a large number of repeated measurements of mixing at short (~ms) time scales. Thus, it was possible to obtain reproducible, time-averaged measurements of mixing that are inaccessible in conventional tracer mixing studies. Finally, through a comparison of the mixing pattern measured using this novel sequence with velocity imaging measurements, a preliminary discussion of the relative influence of different mechanisms of granular mixing has been presented. This work will form the foundation for the development and validation of solids mixing models in fluidized beds.

Acknowledgments

The authors acknowledge the financial support of EPSRC (EP/C547195/1 and GR/S20789/01) and Sutton Seeds for supplying the Myosotis seeds. One of the authors (CRM) would like to acknowledge both Deutscher Akademischer Austauschdienst (DAAD) and the Cambridge European Trust.

References

[1] S.P. Sit, J.R. Grace, Effect of bubble interaction on interphase mass-transfer in gas-fluidized beds, Chem. Eng. Sci. 36 (1981) 327.
[2] P. Rowe, B. Partridge, A. Cheney, G. Henwood, E. Lyall, The mechanics of solids mixing in fluidized beds, Trans. Inst. Chem. Eng. 43 (1965) 271.
[3] I. Eames, M.A. Gilbertson, Mixing and drift in gas-fluidized beds, Powder Tech. 154 (2005) 185.
[4] T. Hayakawa, W. Graham, G.L. Osberg, A resistance probe method for determining local solid mixing rates in a batch fluidized bed, Can. J. Chem. Eng. 42 (1964) 99.
[5] M. Stein, Y.L. Ding, J.P.K. Seville, D.J. Parker, Solids motion in bubbling gas fluidized beds, Chem. Eng. Sci. 55 (2000) 5291.
[6] B. Du, W. Warsito, L.S. Fan, ECT studies of gas–solid fluidized beds of different diameters, Ind. Eng. Chem. Res. 44 (2005) 5020.
[7] P.N. Rowe, C.X.R. Yacono, Bubbling behaviour of fine powders when fluidized, Chem. Eng. Sci. 31 (1976) 1179.
[8] M. Nakagawa, S.A. Altobelli, A. Caprihan, E. Fukushima, E.-K. Jeong, Non-invasive measurements of granular flows by magnetic resonance imaging, Exp. Fluids 16 (1993) 54.
[9] E.E. Ehrichs, H.M. Jaeger, G.S. Karczmar, J.B. Knight, V.Y. Kuperman, S.R. Nagel, Granular convection observed by magnetic–resonance–imaging, Science 267 (1995) 1632.
[10] C. Huan, X.Y. Yang, D. Candela, R.W. Mair, R.L. Walsworth, NMR experiments on a three-dimensional vibrofluidized granular medium, Phys. Rev. E 69 (2004) 041302.
[11] A.C. Rees, J.F. Davidson, J.S. Dennis, P.S. Fennell, L.F. Gladden, A.N. Hayhurst, M.D. Mantle, C.R. Müller, A.J. Sederman, The nature of the flow just above the perforated plate distributor of a gas-fluidized bed, as imaged using Magnetic Resonance, Chem. Eng. Sci. 61 (2006) 5702.
[12] C.R. Müller, J.F. Davidson, J.S. Dennis, P.S. Fennell, L.F. Gladden, A.N. Hayhurst, M.D. Mantle, A.C. Rees, A.J. Sederman, Real-time measurement of bubbling phenomena in a three-dimensional gas-fluidized bed using ultrafast magnetic resonance imaging, Phys. Rev. Lett. 96 (2006) 154504.
[13] C.R. Müller, D.J. Holland, J.F. Davidson, J.S. Dennis, L.F. Gladden, A.N. Hayhurst, M.D. Mantle, A.J. Sederman, Rapid two-dimensional imaging of bubbles and slugs in a three-dimensional, gas–solid, two-phase flow system using ultra-fast magnetic resonance, Phys. Rev. E 75 (2007) 020302.
[14] R. Savelsberg, D.E. Demco, B. Blümich, S. Stapf, Particle motion in gas-fluidized granular systems by pulsed-field gradient nuclear magnetic resonance, Phys. Rev. E 65 (2002) 020301.
[15] S. Harms, S. Stapf, B. Blümich, Application of k- and q-space encoding NMR techniques on granular media in a 3D model fluidized bed reactor, J. Magn. Reson. 178 (2006) 308.
[16] P.S. Fennell, J.F. Davidson, J.S. Dennis, L.F. Gladden, A.N. Hayhurst, M.D. Mantle, C.R. Müller, A.C. Rees, S.A. Scott, A.J. Sederman, A study of the mixing of solids in gas-fluidized beds, using ultra-fast MRI, Chem. Eng. Sci. 60 (2005) 2085.
[17] E. Fukushima, Nuclear magnetic resonance as a tool to study flow, Annu. Rev. Fluid Mech. 31 (1999) 95.
[18] J. Granwehr, E. Harel, S. Han, S. Garcia, A. Pines, P.N. Sen, Y.Q. Song, Time-of-flight flow imaging using NMR remote detection, Phys. Rev. Lett. 95 (2005) 075503.
[19] R.B. Thorpe, J.F. Davidson, M. Pollitt, J. Smith, Maldistribution in fluidized beds, Ind. Eng. Chem. Res. 41 (2002) 5878.
[20] R.M. Cotts, M.J.R. Hoch, T. Sun, J.T. Marker, Pulsed field gradient stimulated echo methods for improved NMR diffusion measurements in heterogenous systems, J. Magn. Reson. 83 (1989) 252.
[21] P.T. Callaghan, Principles of Nuclear Magnetic Resonance Microscopy, Calrendon Press, Oxford, 1991.
[22] J.J. van Deemter, Mixing, in: J.F. Davidson, R. Clift, D. Harrison (Eds.), Fluidization, London, 1985.